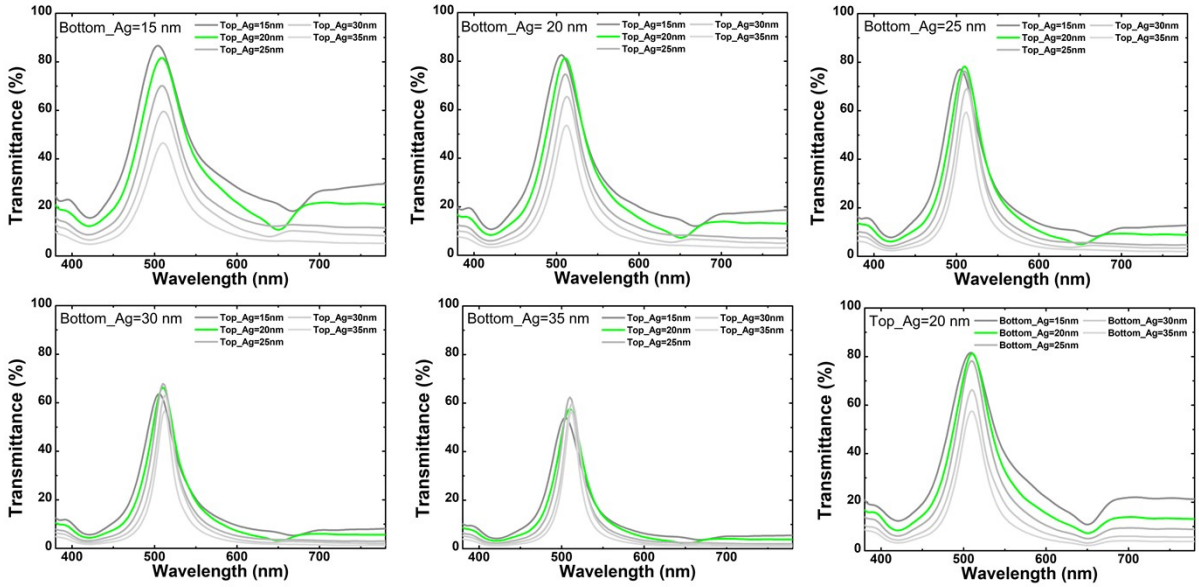

Fig. S1. Spectral properties according to the thickness of Ag reflector.

As the thickness of the Ag reflector layers increases, the transmittance properties of the meta-MIM structure are modified by the inherent trade-off between transparency and reflectivity. As shown in Fig. S1, thicker Ag films yield narrower full width at half maximum (FWHM) values, indicating enhanced spectral selectivity, but at the expense of reduced peak transmittance. Conversely, thinner Ag films provide higher peak transmittance but broaden the resonance, thereby reducing color purity. For the green filter, when both the top and bottom Ag layers are 15 nm, the structure exhibits the highest peak transmittance of 86.66% at 504 nm, albeit with a relatively broad FWHM of 81 nm. By increasing both Ag layers to 20 nm, the peak transmittance decreases slightly to 81.26% at 510 nm, while the FWHM narrows significantly to 60 nm, leading to improved color purity. This corresponds to only a 6.2% reduction in transmittance compared to the thinnest case, whereas the FWHM decreases by 25.9%, which highlights a favorable balance between transmission efficiency and spectral sharpness.

Accordingly, an Ag thickness of 20 nm for both the top and bottom layers was identified as the optimal configuration. This optimization demonstrates that fine-tuning the Ag thickness allows the layers to effectively serve their dual role as partially transparent windows and reflective cavity boundaries, thereby enabling strong resonance intensity and high color purity without compromising device performance.

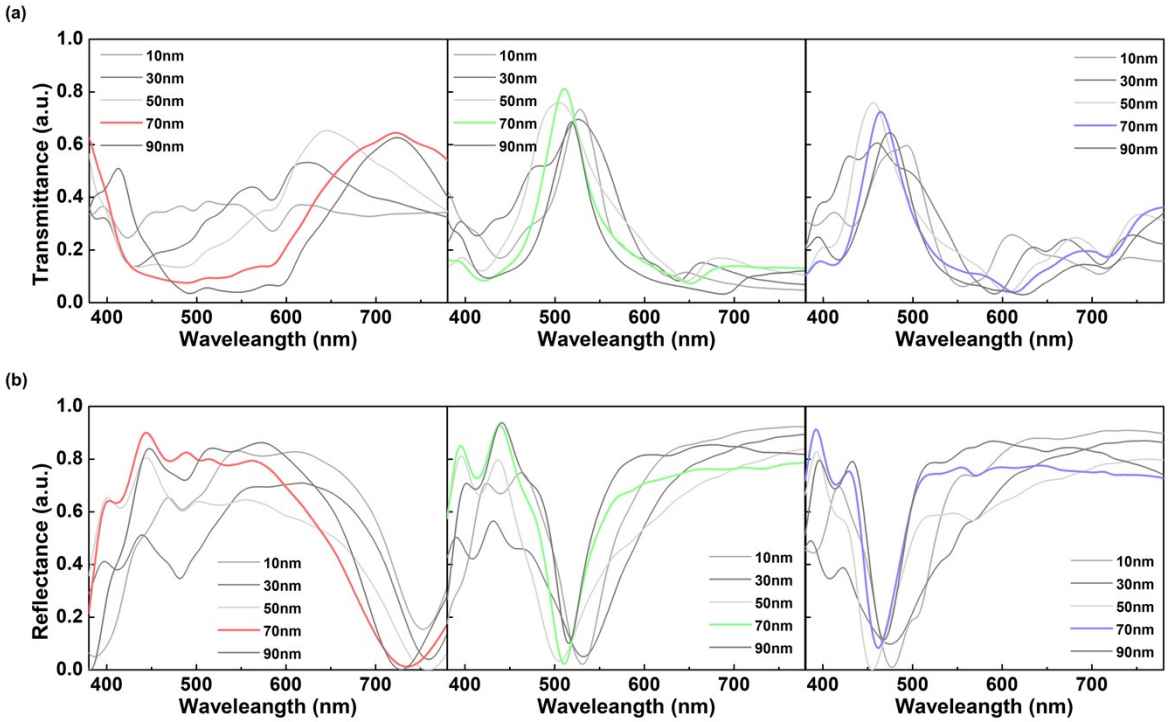

Fig. S2. Spectral properties according to the thickness of outer capping layer. (a) Transmittance. (b) Reflectance.

As the thickness of the outer capping dielectric layer increases, the transmittance properties of the meta-MIM structure are enhanced. As shown in Fig. S2, when the capping layer thickness reaches 70 nm, the RGB device exhibits the highest resonance peak intensity with minimized wavelength shifts. At this optimal thickness, the FWHM is also reduced, indicating improved color purity. The outer capping layer has a negligible influence on the phase difference between the reflective and cavity layers. It significantly enhances impedance matching at the cavity/air interface, thereby facilitating more efficient light extraction. Consequently, reflection losses are suppressed, and the precision of the Fabry–Perot (FP) cavity is improved, leading to an amplified resonance peak without perturbing the intrinsic resonance conditions. As the thickness of the outer capping dielectric layer increases, the optical response of the meta-MIM structure is significantly modified. Fig. S2a presents the transmittance spectra for RGB devices with varying capping thicknesses (10, 30, 50, 70, and 90 nm). When the capping layer thickness reaches 70 nm, all three devices exhibit the highest resonance peak intensities with minimized wavelength shifts. At this condition, the FWHM is also reduced, indicating improved color purity.

To further substantiate this result, Fig. S2b shows the corresponding reflectance spectra. Importantly, for each RGB channel, the capping thickness of ~70 nm yields the lowest reflectance at the resonance wavelength, confirming that this thickness provides the most effective impedance matching at the cavity/air interface. At smaller thicknesses (10–30 nm), incomplete suppression of reflection leads to broadened and weaker resonances, particularly in the red channel. For thicker capping layer (e.g., 90 nm), additional optical path length introduces spectral shifts without further reducing reflection losses. Together, these results confirm that a 70 nm capping layer represents the optimal trade-off between transmittance enhancement, reflectance suppression, and spectral stability. The capping dielectric thus acts as an anti-reflection–like layer, improving optical outcoupling and resonance fidelity without perturbing the intrinsic FP condition.

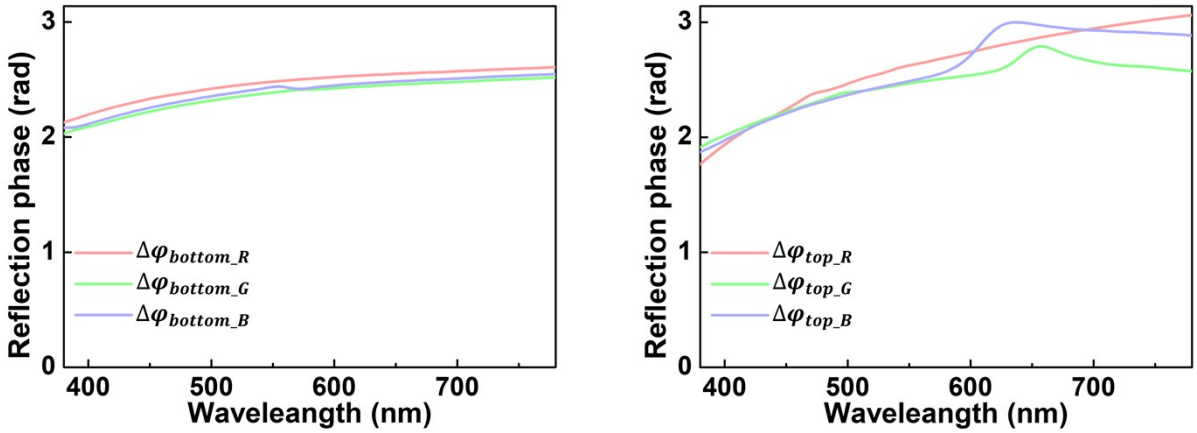

Fig. S3. Wavelength-dependent reflection phases of the Ag–AAO interfaces. (a) Reflection phase at the bottom Ag – AAO interface and (b) at the top Ag – AAO interface for the designed RGB structure.

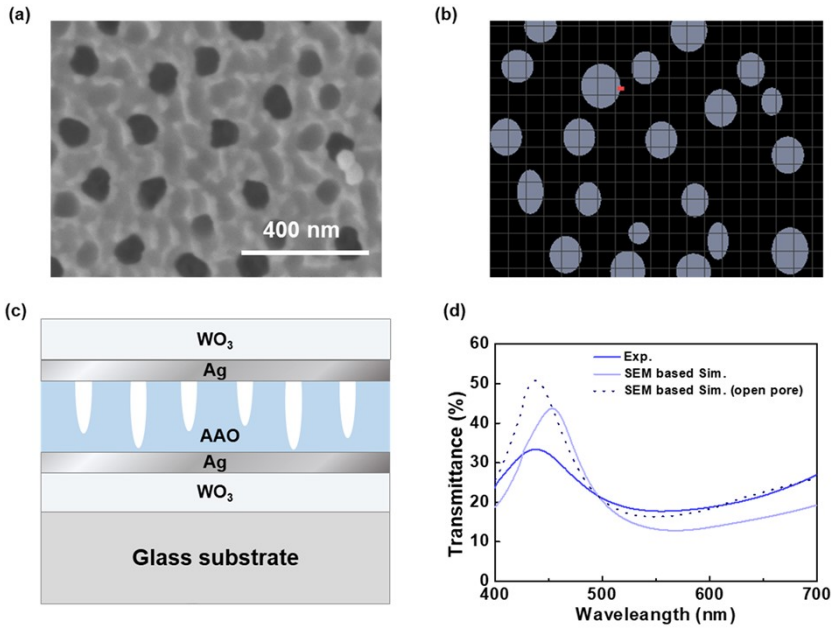

Fig. S4. (a) Top view SEM image of the blue device without the top Ag/WO_3 layers. (b) Hole pattern modeled from the SEM image in (a) for FDTD optical simulation. (c) Cross section view schematic of the blue device without the top Ag/WO_3 layers. (d) Spectral properties measured by a UV-Vis spectrometer and simulated by FDTD. The experimental result (deep blue solid line) is compared with numerical simulations based on the actual SEM-derived geometry (light blue solid line) and a fully perforated idealized structure (light blue dashed line).

As shown in Fig. S4, the FDTD optical simulation results based on SEM-derived structures exhibit better agreement with the experimental data than those based on idealized geometries. This improved correspondence arises from the incorporation of actual morphological features observed in SEM images, such as irregular pore shapes and incomplete hole penetration. To more accurately reflect the real morphology seen in Fig. 4e—where certain nanopores do not fully penetrate through to the bottom Ag layer—a modified FDTD model was constructed by introducing randomly distributed non-penetrating holes with residual thicknesses of approximately 30–50 nm. This modification enabled a more realistic optical response by accounting for the imperfect pore formation commonly found in the fabricated AAO templates. In particular, for the blue device, the simulated resonance wavelength appears at 454 nm, while the experimental value is 432 nm—showing a blue shift of approximately 22 nm, yet preserving the overall spectral shape. The SEM-based simulated peak transmittance was 43.73%, while the experimental value was 33.36%, corresponding to a reduction of 23.7% relative to the simulation results. This discrepancy is primarily attributed to imperfect surface flatness of the AAO layer and the deposited films, which introduce deviations from ideal FP cavity conditions. Additionally, the broader FWHM observed in the experimental spectrum is attributed to thickness non-uniformity and morphological imperfections in the AAO structure, both of which degrade spectral confinement within the resonance cavity. For comparison, a further simulation assuming a fully open pore structure—i.e., complete penetration through the Ag layer using the same pore geometry—was performed and is shown as a dashed line in Fig. S4d. This idealized model predicts a peak at 462 nm with a transmittance of 52.8%, revealing that partial pore closure significantly reduces the resonance strength and induces a spectral blue shift. The comparison clearly underscores the importance of faithfully capturing morphological non-idealities when predicting the optical response of AAO-based photonic

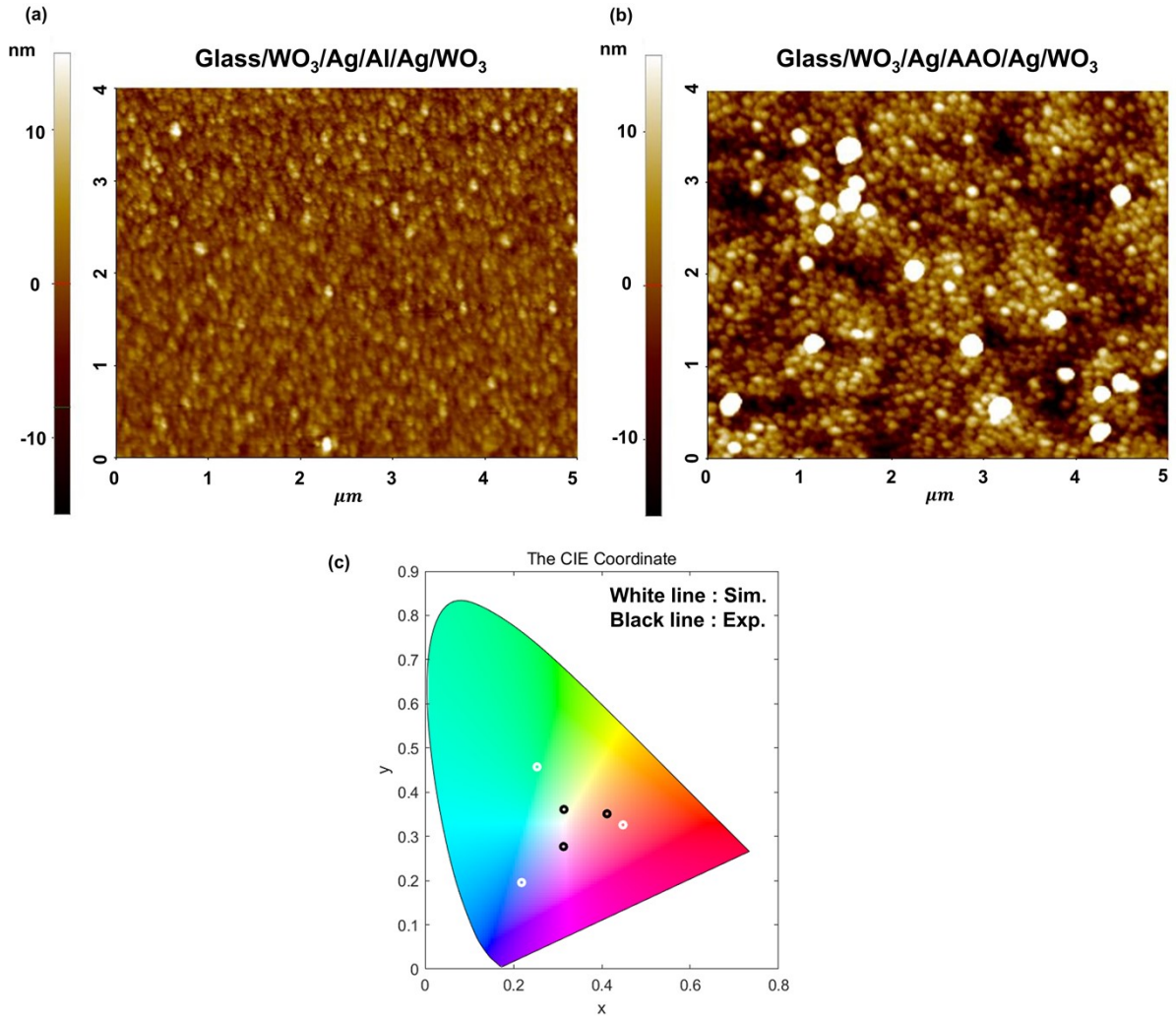

Fig. S5. Comparison of experimental and simulated spectra, surface morphologies, and color coordinates. (a) AFM height image of the fabricated structure without anodization (Substrate/WO_3/Ag/Al/Ag/WO_3). (b) AFM height image of suggested AAO-based device (Substrate/WO_3/Ag/AAO/Ag/WO_3). (c) corresponding CIE 1931 color coordinates.
structures.

The spectral deviation between simulation and experiment mainly originates from the increased surface roughness in the anodized AAO structure. A rougher surface reduces the coherence of the FP cavity and weakens the resonance intensity. Atomic force microscopy (AFM, NX20; Park Systems, Suwon, South Korea) was employed to measure the surface topography. Fig. S5a and b present AFM images: (a) the reference device fabricated without anodization (Substrate/WO_3/Ag/Al/Ag/WO_3) and (b) the proposed AAO-based device (Substrate/WO_3/Ag/AAO/Ag/WO_3). The RMS roughness values are 8.557 nm and 2.516 nm, respectively, demonstrating that the AAO-integrated structure exhibits a significantly rougher surface. This quantitative evidence supports our explanation that surface roughness is the primary reason for the spectral broadening and reduced peak intensity.

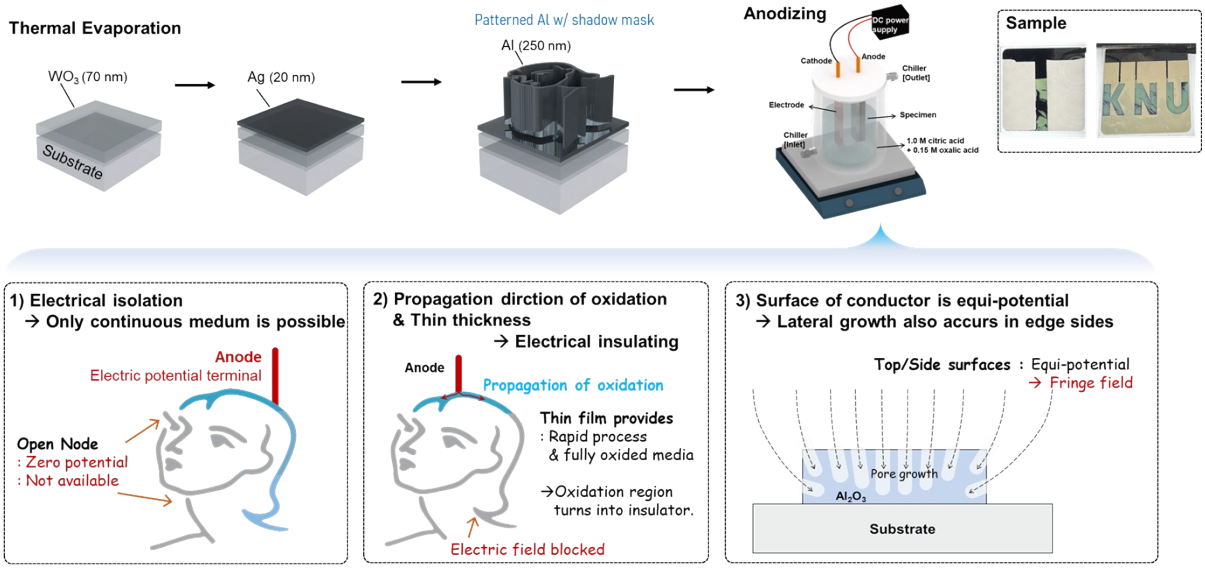

Fig. S6. Fabrication flow and associated issues in patterned thin film Al: 1) Electrical isolation in disconnected patterns resulting in inactive regions; 2) Formation of localized alumina due to rapid top-oxidation and disconnection from underlying Al; 3) Inward oxide growth from pattern edges due to the thinness of the thin film Al layer.

During anodization of thinly patterned aluminum (Al), several critical challenges hinder uniform oxide formation. First, electrically isolated Al patterns prevent current flow, leading to incomplete or absent anodization in those areas. Second, oxidation initiates rapidly from the electrode-connected top surface, often causing premature separation of the Al and limiting alumina formation to only partial regions. Third, due to the characteristic inward growth of alumina within the Al matrix, oxide formation near the pattern edges tends to be significantly thinner, resulting in pronounced non-uniformity across the structure.

For achieving good quality of artwork-liked color generation, the formation of a single continuous Al film design over the whole substrate region is very important. This method ensures adequate electrical continuity, thereby supporting a stable electric field throughout the anodization process. Firstly, if a pattern resembling artwork or a free style is established during Al deposition before anodization, regions with zero potential due to electrical discontinuity will not be accessible for oxidation. Second, the thin film thickness results in the complete oxidation of the Al media, and the process undergoes rapidly. As a result, the Al media transform into insulating media from near positions of the electrode to far positions. This effectively interrupts the electrical pathway. Lastly, given that conductor surfaces are inherently equipotential, the orientation and intensity of the local electric field may become altered near the edges of patterned areas, leading to a lateral growth direction of the pores, as shown in Fig. S6, 3). This degrades the ordering of the pore and consequently reduces the resonance strength.